

# Excited-State Absorption and Circular Dichroism of Ruthenium(II) Tris(phenanthroline) in the Ultraviolet Region

Claire Niezborala and François Hache\*

Laboratoire d'Optique et Biosciences, Ecole Polytechnique, CNRS, INSERM, 91128 Palaiseau Cedex, France

Received: September 22, 2006; In Final Form: June 1, 2007

Excitation of ruthenium(II) tris(phenanthroline) in the visible region results in the transfer of an electron from the central atom toward one of the ligands. To probe this excited state, we have performed pump-induced absorption and circular dichroism in the ultraviolet wavelengths, in the intraligand  $\pi-\pi^*$  transition region. On top of the bleaching of the ground state transitions, new structures appear in the absorption and CD spectra. Thanks to a classical calculation based on the polarizability theory, we can interpret these features as the result of a strong reduction of the excitonic coupling due to a blue shift of the  $\pi-\pi^*$  transition in the reduced ligand accompanied by the onset of new excited-state transitions.

## Introduction

Ruthenium complexes such as ruthenium(II) tris(bipyridyl) and ruthenium(II) tris(phenanthroline) have been extensively studied due to their remarkable properties leading to applications in energy and electron-transfer processes, chemi- and electrochemiluminescent processes and supramolecular assemblies.<sup>1</sup> They are also known to be efficient DNA intercalation compounds<sup>2</sup> and have the characteristics of possessing a high hyperpolarizability envisioning promising optical nonlinear properties,<sup>3</sup> especially under dendritic structures.<sup>4</sup> Most of these applications rely on the metal-to-ligand charge transfer (MLCT) band which lies in the visible region: Upon photon absorption, an electron is transferred from the metal toward the ligands. Consensus now exists that the electron is very rapidly localized on a unique ligand<sup>5</sup> in ruthenium(II) tris(bipyridyl). An identical conclusion holds for ruthenium(II) tris(phenanthroline).<sup>6</sup>

Ruthenium(II) tris(bipyridyl) is an archetype of chiral molecules whose optical activity arises from the excitonic coupling and as such has been a model molecule for the study of new nonlinear chiroptical properties. In particular, the wavelength dependence of the pump-induced circular dichroism (CD) in a pump–probe experiment was thoroughly investigated in the MLCT band.<sup>7</sup> Pump–probe experiments furthermore allow excited-state chiroptical properties to be studied, and pioneering work in this direction was done by Milder et al.<sup>8</sup> Study of the CD of the MLCT band is, however, more complicated than it appears, and Belser et al.<sup>9</sup> have shown that the CD structure in the visible region is not due to coupling of degenerate oscillators, as expected, but the consequence of the coupling of the MLCT transitions with higher-lying ligand transitions. Things are simpler for the ligand transitions taking place in the ultraviolet region. In this spectral range, the CD spectrum displays a strong bisignate structure, which is clearly attributed to the coupling of the degenerate transitions pertaining to the three ligands.<sup>10</sup> Since the seminal work by Bosnich,<sup>11</sup> this bisignate structure has been used to determine the absolute configuration of such metal complexes. It is therefore easier and more informative to study the MLCT state in the ultraviolet region and not in the visible region. Even though optical transitions from the ground

state are well established in the ultraviolet region, it is, however, not the case for the MLCT state. Indeed, excited-state absorption performed in this wavelength range<sup>12</sup> has revealed the onset of several new transitions. In this article, we take advantage of a new pump-induced CD measurement<sup>13</sup> to investigate absorption and CD in the 230–300 nm range after MLCT excitation. Information extracted from the excited-state absorption combined with a simple CD calculation based on the coupled-oscillator model allow us to obtain a clear picture of the CD spectrum of the MLCT state. Two trends are observed: the blue shift of the  $\pi \rightarrow \pi^*$  transition in the reduced ligand which results in a lower efficiency of the coupling with the unperturbed ligands, and the appearance of new  $\pi^* \rightarrow \pi^*$  and ligand-to-metal charge transfer (LMCT) bands with monosignate CD.

## Materials and Methods

The studied sample is a ruthenium(II) tris(1,10-phenanthroline) salt ( $\text{Ru}(\text{phen})_3^{2+}(\text{PF}_6^-)_2$ ) in its racemic and enantiomeric forms. A 150  $\mu\text{M}$  sample in acetonitrile is placed in a 1 mm thick silica cell. Excitation of  $\text{Ru}(\text{phen})_3^{2+}$  is performed by a subpicosecond 400 nm pulse in the MLCT band. Ultrafast spectroscopic experiments have shown that the transferred electron is localized on a single ligand within 300 fs.<sup>14</sup> The first stage is therefore not accessible to our experiment and only the final <sup>3</sup>MLCT state was investigated.

To probe the absorption and the CD in the ligand transitions, a laser source broadly tunable in the far-UV region had to be developed. The experimental setup is based on an amplified 1 kHz titanium-sapphire laser system that delivers 0.8 mJ, 200 fs pulses. These pulses are readily utilized, without any prism or grating dispersion device. The first step to obtain tunable pulses in the UV region is a continuum generation in a 8 mm thick sapphire plate. Such a thick plate was found to yield a more stable continuum. A selected wavelength is then amplified by a two-stage BBO-based noncollinear optical parametric amplifier pumped by the second harmonic of the laser. Selection of the wavelength is obtained by adjustment of the BBO angle and of the pump-signal delay. This setup provides pulses between 500 and 700 nm in the 10  $\mu\text{J}$  range. Two strategies are then used to go to the UV region, either by directly frequency-doubling this signal or by generating the sum-frequency of the signal with a

\* Corresponding author. E-mail: francois.hache@polytechnique.edu.

400 nm pulse. Both processes are performed in a 1 mm thick, type I BBO crystal cut at 60°. The first process is straightforward and provides wavelengths between 250 and 350 nm. The second process is somewhat more complex because it requires a new stage with temporal and spatial overlap of two beams, but it is necessary to go to shorter wavelengths and provides tunability between 220 and 260 nm. Both techniques give similar characteristics. The pulse bandwidth ( $\sim 2$  nm) is mostly limited by the phase-matching condition in the last frequency-doubling or mixing stage. The UV pulse energy is in the nanojoules range, which is sufficient for probe pulses. Pulse duration was estimated from the cross-correlation between the pump and the probe to ca. 800 fs.

Measurement of the excited-state absorption and CD is based on a new technique detailed in ref 13. The general principle is as follows. The sample is placed between a polarizer and a crossed analyzer, and a Babinet–Soleil compensator (BS) is inserted between the sample and the analyzer. Transmission of the probe through the whole setup is monitored by a photomultiplier tube (PMT) as a function of the BS retardation. When the BS is close to the zero retardation position, the PMT signal yields a parabola whose minimum position is closely related to the ground state CD. When the pump is set on the sample, it induces a modification of the PMT signal. To measure this signal change, the pump is modulated with a mechanical chopper and the modulated part of the PMT signal is detected with a lock-in amplifier. Plotting the lock-in amplifier signal as a function of the BS retardation yields a second parabola whose curvature and minimum position straightforwardly give the pump-induced absorption and CD changes. A close examination of the process<sup>13</sup> shows that this technique allows a ratio of the CD change to the absorption change of a few  $10^{-4}$  to be readily detected. It is possible to carry out this experiment as a function of the pump–probe delay and to measure time-resolved absorption and CD with a subpicosecond time resolution. Pump and probe beams are focused with a 250 mm focal length lens onto the sample. The probe energy is kept as low as possible to ensure that no probe-induced effect can happen. The pump energy is about 200 nJ per pulse, leading to the excitation of about 10% of the molecules.

## Results

Prior to the measurements, a preliminary check has been carried out to verify that the two enantiomers yielded opposite results for CD and that no CD was measurable for the racemic mixture. All three samples gave the same pump-induced absorption change as expected. We have therefore concentrated on the  $\Lambda$ -enantiomer; the results can be readily extended to the  $\Delta$ -enantiomer by changing the sign of the CD data. Complete measurements have been performed for 32 wavelengths spanning the 232–303 nm range. Time-resolved measurements did not provide any new information because we could not access the relevant timescales. On the one hand, the molecules undergo a very rapid electronic relaxation from  $^1\text{MLCT}$  to  $^3\text{MLCT}$  after excitation. This process has been measured in the 100 fs range.<sup>14</sup> On the other hand, de-excitation toward the ground state occurs in the microsecond range.<sup>15</sup> Our time scale is too long for the ultrafast electronic changes to be measured and too short to observe recovery of the ground state. We have therefore performed the measurements for a fixed pump–probe delay (50 ps). The results are displayed in Figure 1 where the measured change in absorption and CD are plotted as a function of the probe wavelength. Very nice structures around the ligand absorption band are observed. The absorption change curve

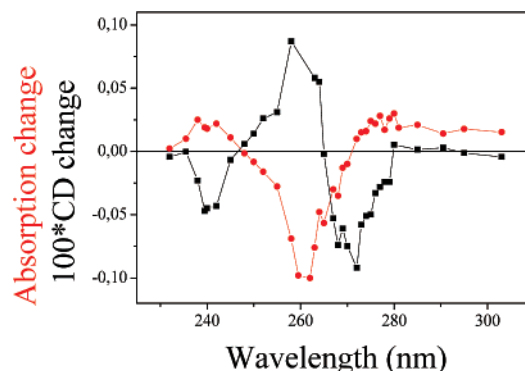


**Figure 1.** Differential absorption (●) and CD (■) spectra of  $\Lambda$ -ru-thenium(II) tris(phenanthroline) measured 50 ps after the excitation of the MLCT band. Absorption and CD are expressed in optical density.

displays a strong bleaching of the ligand absorption band at 260 nm and two induced absorption side bands appear around 240 and 280 nm. Such induced absorption bands have been observed and thoroughly discussed in ref 12. The CD curve also displays a bleaching of the ground state CD accompanied by a new band at 240 nm. These features clearly reflect the change in the electronic structure when passing from the ground to the MLCT state. To gain a deeper insight in the MLCT state, it would be good to obtain its absorption and CD spectra. This operation is, however, quite challenging. Indeed, experimental spectra involve bleaching of the ground transitions as well as onset of new bands and it is very difficult to sort out these contributions experimentally, particularly because of the difficulty of knowing precisely the pump intensity and the proportion of excited molecules.<sup>12</sup> To overcome this problem and to better understand the structure of the MLCT CD spectrum, we have developed a calculation based on the coupled-oscillator model. By fitting together the absorption and CD spectra in the ground-state as well as in the excited state, we are able to decipher the role of the various transitions involved in the MLCT.

## Model Calculation and Discussion

**Ground State.** Unlike the case of the MLCT transition that lies in the visible region and involves nondegenerate couplings,<sup>9</sup> the origin of the CD in the lowest ligand absorption bands of  $\text{Ru}(\text{phen})_3^{2+}$  is well understood and very satisfactorily described by degenerate coupled-oscillator CD.<sup>10</sup> The three equi-energetic excitations, corresponding to processes within each isolated but equivalent phenanthroline ligand, are coupled by dipole–dipole coupling. Within the point group of the chromophore ( $D_3$ ), this results in the creation of eigenstates of  $A_2$  and  $E$  symmetry. These eigenstates are split by the dipole–dipole “exciton” interaction and display equal and opposite rotational strength. This results in a characteristic bisignate excitonic CD. As the excitations are relatively intense and isolated, it is appropriate to neglect the coupling to other (MLCT) excitations in the first approximation.

We have recently developed a CD calculation based on Applequist’s polarizability theory<sup>16</sup> that straightforwardly allows us to simulate the CD spectra for an arbitrary number of (degenerate or nondegenerate) coupled oscillators. Details of the calculation can be found in ref 17. For a given geometric structure of the molecule, inputs for this calculation are the energy, oscillator strength, and dipole moment of each transition. Characteristics of the resultant normal modes (energy, oscillator, and rotational strengths) are readily calculated. Fitting of experimental absorption and CD spectra is then possible,

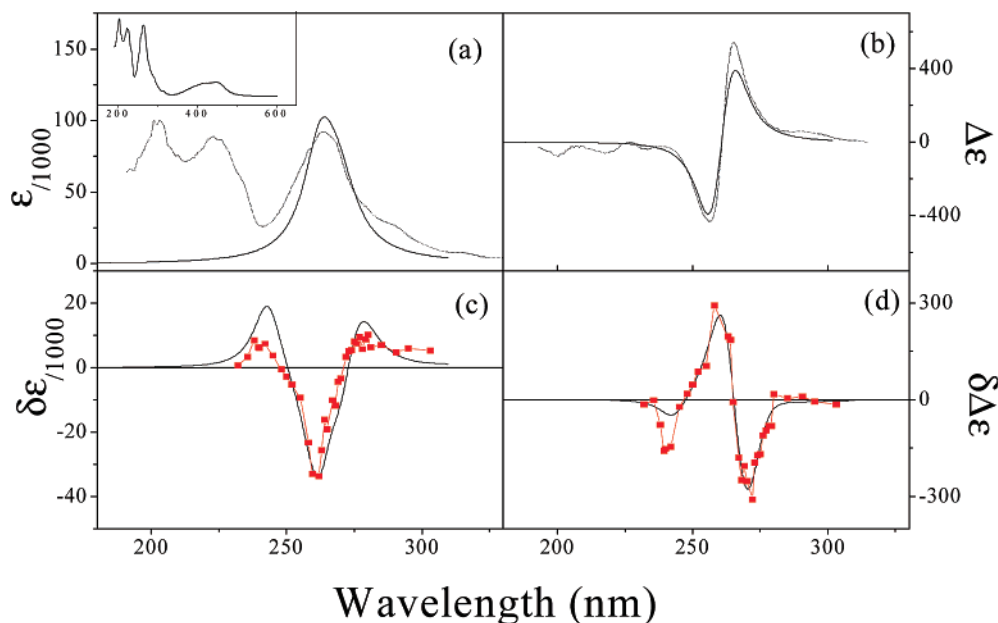


**Figure 2.** (a), (b) Steady-state absorption and CD spectra around the ligand  $\pi-\pi^*$  transitions of  $\Lambda$ -ruthenium(II) tris(phenanthroline). The solid lines are the result of the model calculation. The inset in (a) shows the absorption spectrum on a broader range, including the MLCT transition. (c), (d) Differential absorption and CD spectra, normalized to 100% of excited molecules. The solid squares are experimental data, and the solid lines are theoretical fits. A fraction of 8% of excited molecules is inferred from this adjustment. All ordinates units are  $\text{M}^{-1} \text{cm}^{-1}$ .

	Ligand transitions	Normal modes	$E$	$f$	$R$
Ground state	$\pi^*$ — — — $\pi$ $\uparrow\downarrow$ $\uparrow\downarrow$ $\uparrow\downarrow$		4.72	1.20	-18.4
			4.60	0.30	+ 9.2
MLCT			5.10	0.36	- 1.6
			4.68	0.86	- 8.1
			4.61	0.12	+ 5.4
			4.49	0.48	+ 3.8
			3.10	0.28	+ 0.5

**Figure 3.** Schematic of the ligand transitions introduced in the calculation and the corresponding normal modes for the ground state and the MLCT state. The three columns on the right-hand side display the characteristics of the normal modes:  $E$ , energy in eV;  $f$ , oscillator strength;  $R$ , rotational strength in Debye–Bohr magneton.

provided the introduction of a phenomenological bandwidth for each normal mode.

In Figure 2 a,b, we have applied this calculation to the steady-state absorption and CD spectra of  $\Lambda$ -Ru(phen) $_3^{2+}$ , considering the coupling of three identical oscillators in a  $D_3$  symmetry. The distance between the central metal atom and the ligands was taken at 3.0 Å, in accordance with the Ru(phen) $_3^{2+}$  geometry.<sup>18</sup> The parameters obtained from the fit are the following: transition energy = 4.64 eV, oscillator strength = 0.6. Characteristics of the normal modes are displayed in Figure 3. Inserting a unique bandwidth of 0.28 eV for each transition yields the adjustment of Figure 2a,b. Note that the same parameters are used to recover the correct shape of the absorption and the CD spectra as well as their absolute amplitudes (in  $\text{M}^{-1}\text{cm}^{-1}$ ).

**MLCT State.** Starting from the above calculation, we want now to describe the MLCT state. After excitation of Ru(phen) $_3^{2+}$ , one electron jumps from the metal to one of the

ligands. This means that two out of the three phen ligands are unchanged whereas the third one has been reduced to phen $^-$ . The problem is to obtain a description of the electronic transitions of Ru $^{3+}$ (phen) $_2$ (phen) $^-$ . This issue has been thoroughly addressed in ref 12 where the excited-state absorption of Ru(phen) $_3^{2+}$  has been studied. Three transitions must be considered in the spectral range under consideration. On the one hand, the  $\pi-\pi^*$  transition in the ligand is blue-shifted. Note that this blue shift is in agreement with the geometrical contraction of the phenanthroline ligands upon reduction recently calculated in ref 19. On the other hand, two transitions of the additional electron appear on the red side of the original transition: LMCT and  $\pi^*-\pi^*$ . This latter transition has been observed at 3.1 eV (394 nm).<sup>6</sup> Altogether, we have to consider the coupling of five transitions: the two  $\pi-\pi^*$  transition in the unperturbed phen ligands and the three new transitions in phen $^-$ . We have adjusted these parameters to fit the absorption and the CD changes measured in our experiments (Figure 2c,d).

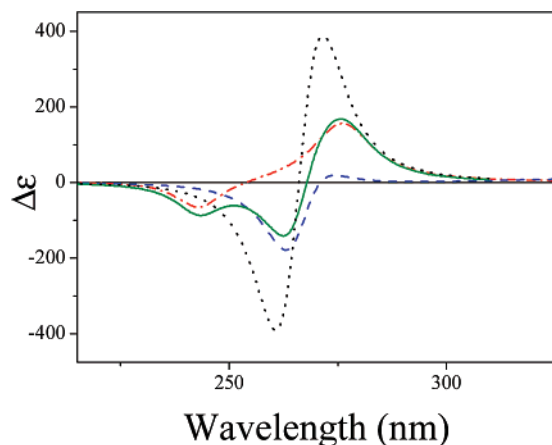


**Figure 4.** Calculated CD spectra: (dotted line) ground state; (solid line) MLCT state. The MLCT spectrum can be decomposed in the unperturbed phen ligand contribution (dashed line) and in the phen<sup>−</sup> contribution (dot-dashed line). Note that the  $\pi^* \rightarrow \pi^*$  transition is out of this frequency range.

Noting  $\eta$ , the fraction of excited molecules, the extinction coefficient of the sample after excitation is

$$\epsilon = (1 - \eta)\epsilon(\text{Ru(phen)}_3^{2+}) + \eta\epsilon(\text{Ru}^{3+}(\text{phen})_2(\text{phen})^-)$$

with obvious notations. The change in  $\epsilon$  therefore reads

$$\delta\epsilon = \eta[\epsilon(\text{Ru(phen)}_3^{2+}) - \epsilon(\text{Ru}^{3+}(\text{phen})_2(\text{phen})^-)]$$

Similar expressions hold for the CD,  $\Delta\epsilon$ . The fits displayed in Figure 2c,d yield a fraction of excited molecules  $\eta = 0.08$ , a value in correct agreement with an estimation obtained from the experimental parameters.

The parameters (energy, oscillator strengths) for the phen<sup>−</sup> transitions are (3.1 eV, 0.3), (4.5 eV, 0.3), and (5.1 eV, 0.3). The oscillator strengths were chosen equal to half the unperturbed ligand ones to take into account the fact that only one electron is involved in these transitions whereas there are two electrons in the unperturbed ligand. The dipole moment for the LMCT transition was supposedly oriented along the line joining the metal to the center of the ligand. The resulting normal modes and their characteristics are depicted in Figure 3; they yield the adjustment of Figure 2c,d. Here again a unique bandwidth of 0.28 eV has been chosen. Note that the major uncertainty on the transition parameters comes from the inability to determine those bandwidths accurately.

Our calculation has the advantage that it provides the CD spectrum of the MLCT state and allows identification of its various components. The results are plotted in Figure 4. The dotted curve corresponds to the ground-state CD whereas the solid curve corresponds to the MLCT CD. This last curve can be decomposed into two contributions: one coming from the unperturbed phen ligands and one coming from the phen<sup>−</sup> ligand. The CD of the unperturbed phen ligands can be understood within the degenerate coupled oscillator model. However, because only two oscillators are coupled, the energy shift as well as the rotational strengths are strongly reduced compared to the ground state case. Furthermore, the two rotational strengths are not perfectly opposite due to the influence of the other levels. On the contrary, the CD of the phen<sup>−</sup> ligand is closer from the nondegenerate coupled oscillator model. The original three transitions experience almost no shift but a rotational strength appears for each, a negative one for the highest ( $\pi \rightarrow \pi^*$ ) transition and two positive ones for the

lowest ( $\pi^* \rightarrow \pi^*$  and LMCT) ones. Note that the  $\pi^* \rightarrow \pi^*$  transition, which takes place at 3.1 eV, is not represented in Figure 4. The total MLCT CD spectrum is the superposition of a bisignate CD structure due to the unperturbed ligand and of three monosignate ones due to the phen<sup>−</sup> ligand. The blue shift of the  $\pi \rightarrow \pi^*$  transition in the reduced phen<sup>−</sup> ligand is responsible for the major change in the MLCT CD. By lifting the degeneracy of the three ligands, it profoundly modifies the coupling conditions and therefore strongly reduces the bisignate CD structure due to excitonic coupling.

## Conclusion

We have carried out measurements of the excited-state absorption and CD spectra of  $\text{Ru(phen)}_3^{2+}$  in the ultraviolet region where the intraligand transitions take place. In agreement with ref 12 we interpret the absorption curves by the onset of three new transitions in the perturbed phen<sup>−</sup> ligand. Thanks to a CD calculation that we have recently developed, this feature allows us to thoroughly understand the structure of the MLCT CD spectrum. It originates in the coupling of two degenerate transitions in the unperturbed phen ligands with the aforementioned three transitions in the phen<sup>−</sup> ligand. The strong excitonic coupling structure observed in the ground state is strongly lowered because of the blue shift of the  $\pi \rightarrow \pi^*$  transition in the reduced ligand.

**Acknowledgment.** We thank Magali Alexandre and Chantal Andraud for providing us with the enantiomerically pure  $\text{Ru(phen)}_3^{2+}$  samples. We are grateful to Professor Serge Fermandjian (Département de Biologie et Pharmacologie Structurales, Institut Gustave Roussy, France) for the steady-state CD measurements.

## References and Notes

- Balzani, V.; Juris, A. *Coord. Chem. Rev.* **2001**, *211*, 97–115.
- Lincoln, P.; Nordén, B. *J. Phys. Chem. B* **1998**, *102*, 9583–9594.
- Dhenaut, C.; Ledoux, I.; Samuel, I. D. W.; Zyss, J.; Bourgalet, M.; Le Bozec, H. *Nature* **1995**, *374*, 339–342.
- Le Boudier, T.; Maury, O.; Bondon, A.; Costuas, K.; Amouyal, E.; Ledoux, I.; Zyss, J.; Le Bozec, H. *J. Am. Chem. Soc.* **2003**, *125*, 12284–12299.
- Riesen, H.; Wallace, L.; Krausz, E. *Inorg. Chem.* **2000**, *39*, 5044–5052.
- Schoonover, J. R.; Omberg, K. M.; Moss, J. A.; Bernhard, S.; Malueg, V. J.; Woodruff, W. H.; Meyer, T. J. *Inorg. Chem.* **1998**, *37*, 2585–2587.
- Mesnil, H.; Schanne-Klein, M.-C.; Hache, F.; Alexandre, M.; Lemercier, G.; Andraud, C. *Phys. Rev. A* **2002**, *66*, 013802 1–9.
- Milder, S. J.; Gold, J. S.; Kliger, D. S. *Chem. Phys. Lett.* **1988**, *144*, 269–272.
- Belser, P.; Daul, C.; Von Zelewsky, A. *Chem. Phys. Lett.* **1981**, *79*, 596–598.
- Rodger, A.; Nordén, B. *Circular dichroism and linear dichroism*; Oxford University Press: Oxford, U.K., 1997.
- Bosnich, B. *Acc. Chem. Res.* **1969**, *2*, 266–273.
- Hauser, A.; Krausz, E. *Chem. Phys. Lett.* **1987**, *138*, 355–360.
- Niezborala, C.; Hache, F. *J. Opt. Soc. Am. B* **2006**, *23*, 2418–2424.
- Yeh, A. T.; Shank, C. V.; McCusker, J. M. *Science* **2000**, *289*, 935–938.
- Van Houten, J.; Watts, R. J. *J. Am. Chem. Soc.* **1976**, *98*, 4853–4858.
- Applequist, J.; Sundberg, K. R.; Olson, M. L.; Weiss, L. C. *J. Chem. Phys.* **1979**, *70*, 1240–1246.
- Dartigalongue, T.; Hache, F. *J. Chem. Phys.* **2005**, *123*, 184901-1/9.
- Buchs, M.; Daul, C. *Chimia* **1998**, *52*, 163–166.
- Shinozaki, K.; Shinozaki, T. *Chem. Phys. Lett.* **2006**, *417*, 111–115.